Ultrafast gaseous "half-wave plate"

P. Béjot, Y. Petit, L. Bonacina, J. Kasparian[#], M. Moret, and J.-P. Wolf[*]

GAP, Université de Genève, 20 rue de l'Ecole de Médecine, CH-1211 Genève 4, Switzerland
[#] Also with Teramobile, Université Lyon 1; CNRS; LASIM UMR 5579, bât. A. Kastler, 43 Bd du 11 novembre 1918, F-69622 Villeurbanne Cedex, France
[*]Corresponding author: jean-pierre.wolf@physics.unige.ch

Abstract: We demonstrate that filaments generated by ultrashort laser pulses can induce a remarkably large birefringence in Argon over its whole length, resulting in an ultrafast "half-wave plate" for a copropagating probe beam. This birefringence originates from the difference between the nonlinear refractive indices induced by the filament on the axes parallel and orthogonal to its polarization. An angle of 45° between the filament and the probe polarizations allows the realization of ultrafast Kerr-gates, with a switching time ultimately limited by the duration of the filamenting pulse.

OCIS codes: (140.7090) Ultrafast lasers; (190.7110) Ultrafast nonlinear optics; (260.1440) Birefringence; (190.3270) Kerr effect; (190.5940) Self-action effects

References and links

1. A. Braun, G. Korn, X. Liu, D. Du, J. Squier, and G. Mourou, "Self-channeling of high-peak-power femtosecond laser pulses in air," Opt. Lett. **20**, 73-75 (1995).
2. S. L. Chin, S. A. Hosseini, W. Liu, Q. Luo, F. Theberge, N. Akozbek, A. Becker, V. P. Kandidov, O. G. Kosareva, and H. Schroeder, "The propagation of powerful femtosecond laser pulses in optical media: physics, applications, and new challenges," Can. J. Phys. **83**, 863-905 (2005).
3. L. Bergé, S. Skupin, R. Nuter, J. Kasparian, and J.-P. Wolf, "Ultrashort filaments of light in weakly-ionized, optically-transparent media," Rep. Prog. Phys. **70**, 1633-1713 (2007).
4. A. Couairon and A. Mysyrowicz, "Femtosecond filamentation in transparent media," Phys. Rep. **441**, 47-189 (2007).
5. J. Kasparian and J.-P. Wolf, "Physics and applications of atmospheric nonlinear optics and filamentation," Opt. Express **16**, 466-493 (2008).
6. J. Kasparian, M. Rodriguez, G. Méjean, J. Yu, E. Salmon, H. Wille, R. Bourayou, S. Frey, Y.-B. André, A. Mysyrowicz, R. Sauerbrey, J.-P. Wolf, and L. Wöste, "White-Light Filaments for Atmospheric Analysis," Science **301**, 61-64 (2003).
7. J. Kasparian, R. Ackermann, Y.-B. André, G. Méchain, G. Méjean, B. Prade, P. Rohwetter, E. Salmon, K. Stelmaszczyk, J. Yu, A. Mysyrowicz, R. Sauerbrey, L. Wöste, and J.-P. Wolf, "Electric events synchronized with laser filaments in thunderclouds," Opt. Express **16**, 5757 (2008).
8. C. P. Hauri, W. Kornelis, F. W. Helbing, A. Couairon, A. Mysyrowicz, J. Biegleert, and U. Keller, "Generation of intense, carrier-envelope phase-locked few-cycle laser pulses through filamentation," Appl. Phys. B **79**, 673-677 (2004).
9. S. A. Trushin, K. Kosma, W. Fuss, and W. E. Schmid, "Sub-10-fs supercontinuum radiation generated by filamentation of few-cycle 800 nm pulses in argon," Opt. Lett. **32**, 2432-2434 (2007).
10. S. Petit, A. Talebpour, A. Proulx, and S. L. Chin, "Polarization dependence of the propagation of intense laser pulses in air," Opt. Commun. **175**, 323-327 (2000).
11. G. Fibich and B. Ilan, "Self-focusing of circularly polarized beams," Phys. Rev. E **67,** 036622 (2003).
12. H. Yang, J. Zhang, Q. J. Zhang, Z. Q. Hao, Y. T. Li, Z. Y. Zheng, Z. H. Wang, Q. L. Dong, X. Lu, Z. Y.Wei, Z. M. Sheng, J. Yu, and W. Yu, "Polarization-dependent supercontinuum generation from light filaments in air," Opt. Lett. **30**, 534-536 (2005).
13. M. Kolesik, J. V. Moloney, and E. M. Wright, "Polarization dynamics of femtosecond pulses propagating in air," Phys. Rev. E **64**, 046607 (2001).
14. S. Tzortzakis, B. Prade, M. Franco, and A. Mysyrowicz, "Time evolution of the plasma channel at the trail of a self-guided IR femtosecond laser pulse in air," Opt. Commun. **181**, 123-127 (2000).
15. J. P. Geindre, P. Audebert, A. Rousse, F. Fallies, J. C. Gauthier, A. Mysyrowicz, A. Dossantos, and G. Hamoniaux, "Frequency-Domain Interferometer for Measuring the Phase and Amplitude of a Femtosecond Pulse Probing a Laser-Produced Plasma," Opt. Lett. **19**, 1997-1999 (1994).
16. Y. H. Chen, S. Varma, I. Alexeev, and H. M. Milchberg, "Measurement of transient nonlinear refractive index in gases using xenon supercontinuum single-shot spectral interferometry," Opt. Express **15**, 7458-7467 (2007).

#93971 - $15.00 USD Received 17 Mar 2008; revised 18 Apr 2008; accepted 20 Apr 2008; published 9 May 2008

17. M. Mlejnek, E. M. Wright, and J. V. Moloney, "Femtosecond pulse propagation in argon: A pressure dependence study," Phys. Rev. E **58**, 4903-4910 (1998).
18. P. Béjot, C. Bonnet, V. Boutou, and J.-P. Wolf, "Laser noise compression by filamentation at 400 nm in argon," Opt. Express **15**, 13295-13309 (2007).
19. G. P. Agrawal, *Nonlinear Fiber Optics* (Academic Press, San Diego, 2001).
20. J. Kasparian, R. Sauerbrey, and S. L. Chin, "The critical laser intensity of self-guided light filaments in air," Appl. Phys. B **71**, 877-879 (2000).
21. P. Sprangle, E. Esarey, and B. Hafizi, "Propagation and stability of intense laser pulses in partially stripped plasmas," Phys. Rev. E **56**, 5894-5907 (1997)
22. A. Becker, N. Aközbek, K. Vijayalakshmi, E. Oral, C. M. Bowden, and S. L. Chin, "Intensity clamping and re-focusing of intense femtosecond laser pulses in nitrogen molecular gas," Appl. Phys. B **73**, 287-290 (2001).
23. B. La Fontaine, F. Vidal, Z. Jiang, C. Y. Chien, D. Comtois, A. Desparois, T. W. Johnson, J.-C. Kieffer, and H. Pépin, "Filamentation of ultrashort pulse laser beams resulting from their propagation over long distances in air," Phys. plasmas **6**, 1615-1621 (1999).
24. M. Rodriguez, R. Bourayou, G. Méjean, J. Kasparian, J. Yu, E. Salmon, A. Scholz, B. Stecklum, J. Eislöffel, U. Laux, A. P. Hatzes, R. Sauerbrey, L. Wöste, and J.-P. Wolf, "Kilometer-range non-linear propagation of femtosecond laser pulses," Phys. Rev. E **69**, 036607 (2004).
25. G. Méchain, A. Couairon, Y.-B. André, C. D'amico, M. Franco, B. Prade, S. Tzortzakis, A. Mysyrowicz, and R. Sauerbrey, "Long-range self-channeling of infrared laser pulses in air: a new propagation regime without ionization," Appl. Phys. B **79**, 379 (2004).
26. G. Méjean, J. Kasparian, J. Yu, E. Salmon, S. Frey, J.-P. Wolf, S. Skupin, A. Vinçotte, R. Nuter, S. Champeaux, and L. Bergé, "Multifilamentation transmission through fog," Phys. Rev. E **72**, 026611 (2005).
27. G. Méchain, G. Méjean, R. Ackermann, P. Rohwetter, Y.-B. André, J. Kasparian, B. Prade, K. Stelmaszczyk, J. Yu, E. Salmon, W. Winn, L. A. V. Schlie, A. Mysyrowicz, R. Sauerbrey, L. Wöste, and J.-P. Wolf, "Propagation of fs-TW laser filaments in adverse atmospheric conditions," Appl. Phys. B **80**, 785-789 (2005).
28. R. Salamé, N. Lascoux, E. Salmon, J. Kasparian, and J. P. Wolf, "Propagation of laser filaments through an extended turbulent region," Appl. Phys. Lett. **91**, 171106 (2007).

1. Introduction

The propagation of laser filaments in gases is now well understood as a dynamic balance between Kerr self-focusing and defocusing on laser-generated plasma [1-5]. Filaments have been characterized in detail in many regards, in particular from the spectral, temporal and spatial point of view. They are able to deliver high intensities (several 10^{13} W/cm^2) over distances far beyond the diffraction limit, therefore providing unique capabilities for applications like atmospheric remote sensing [6], lightning control [7] or few-cycle pulses generation [8, 9].

However, polarization has been left apart in the investigations to date, except for a few pioneering works [10-13] dealing with the influence of the incident polarization on the filament themselves. Studies of filament-induced changes in the refractive index of air have only considered long-lasting effects (nanoseconds to microseconds) of the plasma left behind the pulse [14, 15]. Self-induced birefringence has been observed to generate refractive index changes Δn in the 10^{-5} range [16] for ultrashort lasers focused into gases. The resulting phase shift remains, however, marginal as diffraction restricts the effect to a Rayleigh length of about 100 µm around the beam waist position. In this Letter, we demonstrate that the unique interaction length and the high-intensity conveyed by laser filaments in a rare gas, namely Argon, are sufficient to induce a "half-wave plate" effect, rotating the incident linear polarization of a non-filamenting probe pulse by an arbitrarily selected angle.

2. Experimental setup and numerical methods

A sketch of the experiment is displayed in Fig. 1. Slightly chirped driving (800 nm, 1 mJ, 100 fs) and probe (400 nm, 1 µJ, 100 fs) pulses, both linearly polarized and slightly focused (f = 1 m), propagate collinearly in an Argon-filled cell of 2 m length. While the driving pulse generates a single filament, the probe pulse propagates linearly in absence of the driving pulse. The relative delay between the two pulses can be adjusted by a delay line. The zero delay was determined using a sum-frequency autocorrelation. A zero-order half-wave plate is

#93971 - $15.00 USD Received 17 Mar 2008; revised 18 Apr 2008; accepted 20 Apr 2008; published 9 May 2008

used to set the input polarization of the driving pulse, taken as the reference (**x** axis, $\theta = 0°$). At the output of the cell, the intensity of a small portion of the probe beam is selected by a pinhole (1 mm diameter) to avoid birefringence inhomogeneities related to the beam intensity transverse profile, and measured through a polarizer (Glan cube). The time-integrated signal, as a function of the polarizer orientation, bears both the ellipticity and the polarization axis of the output probe pulse. In particular, a linear polarization appears as a squared cosine function.

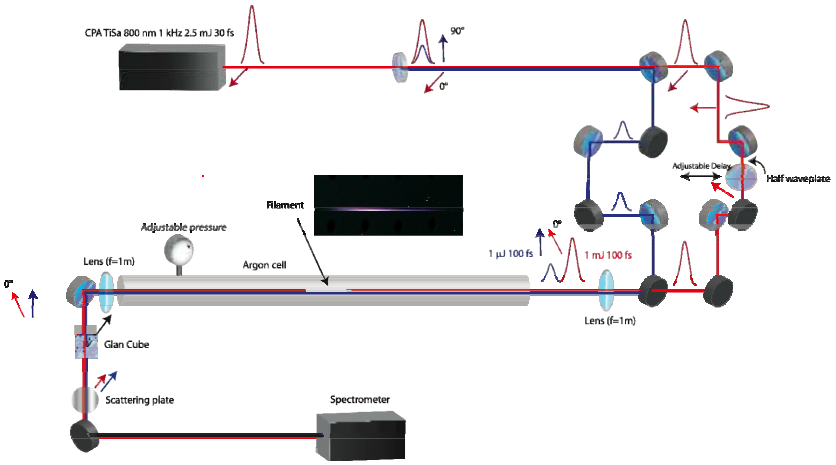

Fig. 1. Experimental setup. The polarization of the driving pulse (filamenting pulse, red) is set relative to that of the probe pulse (blue) before their interaction in the Argon cell. The driving and the probe beams are separated by a spectrometer and their polarization is analyzed by rotating a Glan cube.

We also compare the experimental results with numerical simulations based on a 2D+1 model, where the scalar envelope $\varepsilon = \varepsilon(r, z, t)$, with cylindrical symmetry around the propagation axis, evolves according to the Non-Linear Schrödinger Equation (NLSE) as derived by Mlejnek *et al*. [17]:

$$\partial_z \varepsilon = \frac{i}{2k_0}\Delta_\perp^2 \varepsilon - \frac{ik''}{2}\partial_t^2 \varepsilon + \frac{ik_0 n_2}{n_0}|\varepsilon|^2 \varepsilon - \frac{ik_0}{2n_0^2 \rho_c}\rho\varepsilon - \frac{1}{2}\sigma\rho\varepsilon - \frac{\beta^K}{2}|\varepsilon|^{2K-2}\varepsilon \qquad (1)$$

where t refers to the retarded time in the reference frame $t \to t - z/v_g$ of the pulse with v_g corresponding to the group velocity of the carrier envelope. The terms on the right-hand side of the equation account for spatial diffraction, second order dispersion, instantaneous Kerr effect, plasma defocusing through refraction, absorption, and losses due to multiphoton absorption, respectively. $\rho_c = \omega_0 m_e \varepsilon_0 / e^2$ corresponds to the critical plasma density above which the plasma becomes opaque (1.7×10^{21} cm^{-3} at 800 nm). In addition, the constant $\sigma = ke^2\tau / (\omega m_e \varepsilon_0 (1 + \omega^2\tau^2))$ represents the cross-section for electron-neutral inverse Bremsstralung (τ is the electron-atom relaxation time constant) and β^K corresponds to the coefficient of multiphoton absorption, K being the minimal number of photons necessary to ionize the medium, Argon in our case. β^K is expressed as $\beta^K = \hbar K \omega_0 \rho_{at} \sigma_K$ where ρ_{at} is the Argon density, n_2 is the non-linear refractive index of Argon (at 1 atm, $n_2 = 3.2 \times 10^{-19}$ cm^2/W at 800 nm and $n_2 = 4.9 \times 10^{-19}$ cm^2/W at 400 nm) and σ_K is the multiphoton ionization cross-section. The dynamics of the electric field is coupled to the plasma density ρ by the multiphoton ionization process. The Argon ionization follows the equation:

#93971 - $15.00 USD Received 17 Mar 2008; revised 18 Apr 2008; accepted 20 Apr 2008; published 9 May 2008

$$\partial_t \rho = \sigma_K (\rho_{at} - \rho) |\varepsilon|^{2K} + \frac{\sigma}{U_i} \rho |\varepsilon|^2 - \alpha \rho^2 \tag{2}$$

By numerically solving the NLSE with a Fourier Split-Step scheme in a fully implicit method [18] with input parameters corresponding to our experiment ($E = 750\ \mu J$, $\Delta t_{FWHM} = 30$ fs, and a residual chirp of 330 fs^2), we calculated the evolution of the pulse intensity profile as a function of propagation distance z for each considered Argon pressure.

3. Results and discussion

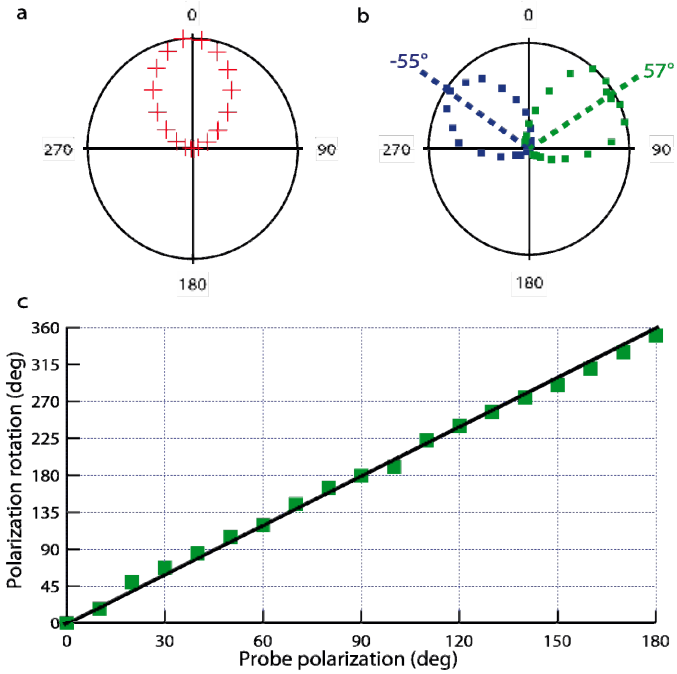

Fig. 2. Filament-induced birefringence leading to a half-wave plate behavior in 3-bar Argon. (a)-(b) Polar plot of the intensity transmitted as a function of the analyzing polarizer angle. For clarity, only half of the pattern is shown, the other half being given by symmetry. (a) Driving pulse (filament) polarization set at 0°. (b) Input (blue, -55°) and output (green, 57°) polarizations of the probe pulse. Co-propagation with the filament rotates the probe polarization by 112°. The squared *cosine* patterns are signatures for linearly polarized light (c) Experimental rotation of the probe polarization as a function of its initial value (green dots): The influence of the filament-induced effective $\lambda_{probe}/2.1$ plate agrees remarkably well with the behavior of an ideal half-wave plate, displayed for reference (solid line).

Figure 2 illustrates the experimentally measured alteration of the probe beam polarization at the exit of the cell (filled with 3 bars Argon) when its initial polarization is set at -55° with respect to the driving beam polarization and the two pulses temporally overlap. After the interaction, the probe beam polarization remains highly linear with a contrast ratio $(I_{\max}^{probe} - I_{\min}^{probe})/(I_{\max}^{probe} + I_{\min}^{probe})$ as high as 98.4%, but rotated to 57±2°, symmetrical to the initial one with regard to that of the filamenting pump beam. This probe polarization flipping is the same as would be expected with a half-wave plate inserted in the probe beam path with its neutral axis at 0°. More precisely, the observed filament-induced birefringence corresponds to a $\lambda_{probe}/2.1$ "waveplate", *i.e.* the difference in the optical paths between the parallel and the perpendicular components of the probe beam amounts 1/2.1 optical cycle. Such a remarkably large dephasing therefore provides a way to tilt the linear polarization of an ultrashort laser

#93971 - $15.00 USD Received 17 Mar 2008; revised 18 Apr 2008; accepted 20 Apr 2008; published 9 May 2008

pulse by a controlled amount: The angle of rotation of the probe polarization is twice the angle that is initially set between the input probe pulse polarization and the driving beam polarization, which undergoes filamentation, as shown in Fig 2(c). Notice, in particular, that choosing a 45° angle between the polarizations of the driving and probe beams flips the probe polarization by 90° at the cell exit. Setting the polarizer perpendicular to the initial probe polarization allows then to switch the probe beam intensity on and off.

The polarization of the probe pulse is only affected within a short range of time delays between the two pulses (200 fs), corresponding to the measured cross-correlation between the pump undergoing filamentation and the probe beam. The effect is maximum when the two pulses temporally overlap. This observation is consistent with the fact that the optical Kerr effect in a monoatomic rare gas like Argon is instantaneous. The duration of the observed "filament-induced Kerr gate" is thus fully controlled by that of the driving laser pulse. Further experiments using few-cycle pulses as driving lasers could therefore lead to optical gates with unprecedented time resolution.

The mechanism of the observed filament-induced birefringence can be explained by the difference in the non-linear refractive indices generated by the driving laser pulse along its polarization axis and the orthogonal axis, respectively. More precisely, the driving field $E^{filament}$, polarized along the **x**-axis (therefore implying $E_y^{filament} = 0$), induces a symmetry breaking in the optical response of the isotropic Argon gas. The non-linear Kerr polarizations of the probe beam along **x** and **y** respectively read [19]:

$$P_{XPM,x}^{probe} = \frac{3\varepsilon_0}{2}\chi_{xxxx}^{(3)}\left|E_x^{filament}\right|^2 E_x^{probe} \tag{3}$$

$$P_{XPM,y}^{probe} = \frac{3\varepsilon_0}{2}\chi_{yyxx}^{(3)}\left|E_x^{filament}\right|^2 E_y^{probe} \tag{4}$$

where XPM stands for the probe Cross-Phase Modulation induced by the filamenting pulse, and the non-linear elements $\chi_{ijkl}^{(3)} = \chi_{ijkl}^{(3)}(\lambda_{probe};\lambda_{probe},\lambda_{pump},-\lambda_{pump})$ are related to the considered cross-Kerr process. All the other non-linear Kerr polarization terms are negligible here, as the ratio of the probe and driving beam energies is 10^{-3}. As the dominant contribution to the $\chi^{(3)}$ tensor in atomic gases like Argon is governed by the electronic cloud response (*i.e.* by the atomic nonlinear polarizability), and since the filament and probe frequencies are far from any resonant transition of Argon, we can consider that $\chi_{xxxx}^{(3)} = 3\chi_{yyxx}^{(3)}$ [19]. As a consequence, the filament-induced birefringence is:

$$\Delta n_{XPM}^{probe} = \frac{1}{2n_0}\left(\frac{3}{2}\mathrm{Re}\left(\chi_{xxxx}^{(3)} - \chi_{xxyy}^{(3)}\right)\right)\left|E_x^{filament}\right|^2 = n_2^{XPM} I^{filament} \tag{5}$$

with

$$n_2^{XPM} = \mathrm{Re}\left(\chi_{xxxx}^{(3)}\right)\Big/\left(n_0^2\varepsilon_0 c\right) = 4n_2\Big/3 \tag{6}$$

Here, n_2^{XPM} is the XPM non-linear refractive index of Argon, $I^{filament}$ the intensity within the filament, n_0 = 1.0003 the linear refractive index of Argon at the probe frequency for experimental pressures at room temperature, ε_0 the vacuum permittivity and c the speed of light in vacuum. n_2 is the "usual" non-linear refractive index as used *e.g.* in Eq. (1). Integrated over the whole interaction length, this birefringence induces a dephasing between the probe beam components along the fast and slow polarization axes of:

$$\Delta\varphi_{XPM}^{probe} = 2\pi\int \Delta n_{XPM}^{probe}\,dz\Big/\lambda_{probe} = 2\pi n_2^{XPM}\int I^{filament}(z)dz\Big/\lambda_{probe} \tag{7}$$

#93971 - $15.00 USD Received 17 Mar 2008; revised 18 Apr 2008; accepted 20 Apr 2008; published 9 May 2008

As is usual in filamentation models, the third-order susceptibility of the plasma (ions and electrons) is not taken into account, because (i) electrons only have a significant contribution in the relativistic regime [20] and (ii) the small relative abundance of ions relative to neutral molecules (typically 10^{-4} [21]) and the fact that their third-order susceptibility is smaller than that of neutrals and does not deviate by more than one order of magnitude [20] prevents them from having any measurable contribution.

$\Delta\varphi_{XPM}^{probe}$ varies with the nonlinear refractive index n_2^{XPM}, and hence, with the Argon pressure in the cell at a fixed temperature. The measured birefringence at different Argon pressures is presented in Fig. 3 and Fig. 4. As described above, a pressure close to 3 bars (precisely 3.3±0.2 bars) permits to generate an ideal half-wave plate. For lower pressures, an elliptic polarization is observed. A fit of the angular pattern of the output polarization (Figs. 3(b)-3(d)) yields a contrast ratio of 67.7% at 1 bar, 39.5% at 2 bar and 98.4% at 3 bar, as well as the orientation of their ellipticity main axis, which amounts to -51±3°, 71±5° and 57±2° respectively. This elliptical polarization is the signature for a smaller dephasing $\Delta\varphi_{XPM}^{probe}$, corresponding to $\lambda_{probe}/8.3$ at 1 bar and $\lambda_{probe}/3.4$ at 2 bar, respectively, Fig. 5(a).

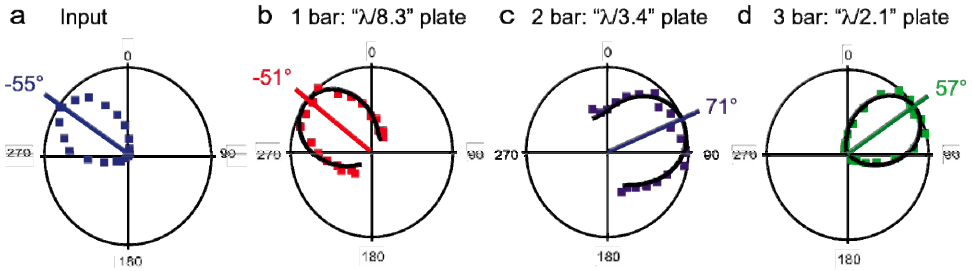

Fig. 3. Pressure dependence of the filament-induced birefringence. (a). Input probe polarization; (b)-(d). Output probe beam polarization for 1, 2 and 3 bar respectively. The black solid lines are fits assuming elliptical polarizations.

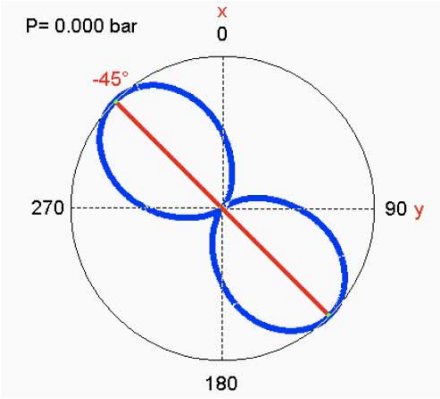

Fig. 4. (1.3 MB) Movie of the pressure dependence of the output polarization diagram of a probe beam driven by an ultrashort laser filament. The movie displays, for each pressure, the simulated signal of the probe beam as a function of the orientation of a polarizer downstream of the interaction region between the drive and pump pulses.

To gain more insight into the pressure dependence, we compared the experimental results with the output of the numerical simulations providing the longitudinal intensity profile at the different pressures, and thus the corresponding birefringence Δn_{XPM}^{probe} through Eq. (5). This dephasing depends linearly on the Argon pressure, in excellent agreement with the experimental data (Fig. 5(a)) for a value of n_2^{XPM} proportional to the Argon pressure and equal

#93971 - $15.00 USD Received 17 Mar 2008; revised 18 Apr 2008; accepted 20 Apr 2008; published 9 May 2008

to 1.6 x 10^{-20} cm^2/W at 1 atm. This value lies below that expected from Eq. (6). Such underestimation is due to the fact that the calculations overestimate the pump intensity, because they consider that of the beam center while the actual intensity is lower in the beam region selected by the pinhole. Further work is required to provide a quantitative transverse profile of filament-induced birefringence and achieve a better quantitative agreement.

As can be seen on Fig. 5(b), our simulations show that higher pressures (*i.e.* higher n_2^{SPM} values) result in longer filaments with lower intensity clamping [21, 22]. These opposite effects roughly compensate each other when calculating the integral $\int I^{filament}(z)dz$, so that the dephasing $\Delta\varphi_{XPM}^{probe} = 2\pi n_2^{XPM} \int I^{filament}(z)dz \Big/ \lambda_{probe}$ varies like n_2^{XPM}, *i.e.* with the Argon pressure.

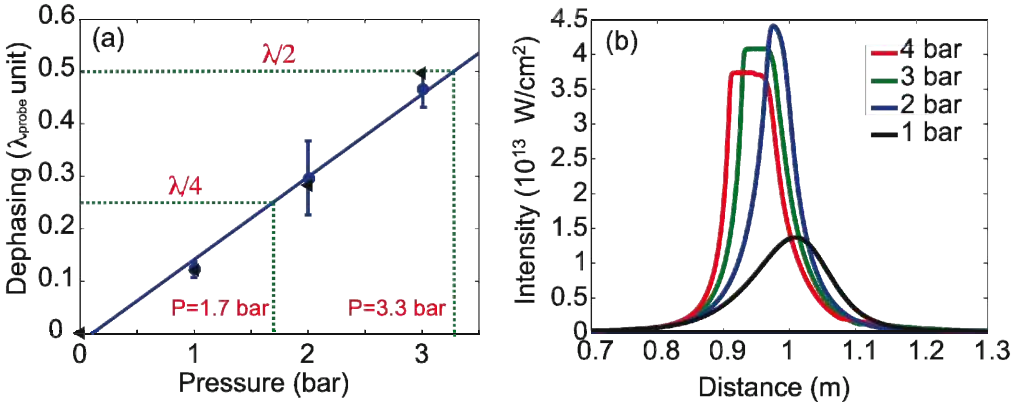

Fig. 5. (a). Experimental (circles) and simulated (triangular) pressure dependence of the filament-induced dephasing. (b). Evolution of the intensity at the filament center with the propagation distance, depending on the pressure.

As the dephasing depends monotonically on the pressure, any $\Delta\varphi_{XPM}^{probe}$ value may be generated by choosing an adequate Argon pressure. For example, an interpolation of the experimental data presented in Fig. 5 suggests that an equivalent "λ/4 plate" can be generated for 1.7±0.1 bar. Even further tuning of the birefringence could be obtained by a careful choice of the investigated position within the beam profile, because of the transverse intensity gradients which are expected to generate transverse birefringence variations.

Conclusion

In conclusion, we have demonstrated that laser-generated self-guided filaments can induce substantial birefringence in near-atmospheric pressure gases. An angle of 45° between the filament and the probe polarizations allows the realization of Kerr-gates, with an unprecedented switching time ultimately limited by the duration of the filamenting pulse. An optical ultrafast switch could even be initiated remotely by self-guided filaments in the atmosphere [6, 23-25], even in perturbed conditions [26-28], opening new perspectives for remote optical ultrafast data transmission and processing, *e.g.* remote ultrafast optical logical gates.

Acknowledgments

This work was supported by the Swiss NSF (contract 200021-111688 and R'equip program), and the Swiss SER in the framework of COST P18 action C06.0114, as well as the Boninchi and Schmideiny foundations.

#93971 - $15.00 USD Received 17 Mar 2008; revised 18 Apr 2008; accepted 20 Apr 2008; published 9 May 2008